PIV wake survey of a drone propeller for amphibious applications

PIV wake survey of a drone propeller for amphibious applications

Silvano Grizzi[1]*, Massimo Falchi[1], Edoardo Martellini[2], Giovanni Aloisio[1], Tiziano Pagliaroli[1-2]

[1]National Research Council – Institute of Marine Engineering (CNR-INM), Via di Vallerano, 139, 00128 Rome, Italy

[2]University Niccolò Cusano, Via Don Carlo Gnocchi 3, 00166 Rome, Italy

ORCID ID:

Silvano Grizzi:	0000-0002-8681-5432
Massimo Falchi:	0000-0001-5396-1743
Edoardo Martellini:	0000-0002-3675-0714
Giovanni Aloisio:	0000-0002-9967-6611
Tiziano Pagliaroli:	0000-0001-9177-3874

*Email: silvano.grizzi@cnr.it

Abstract. Aerial and underwater drones are one of the most attractive technologies to a large number of applications, extending from surveillance of natural reserves to the monitoring of structures. For these reasons, innovative and uncommon applications are constantly appearing. Within this context, drones capable to operate continuously and efficiently in air and water can extend the standard aerial capabilities allowing underwater inspections of harbour structures, pipelines or marine reserves. For this reason, an attractive characteristic for drones is the capability to manoeuvre in different fluids as air and water. This article presents an experimental campaign, carried out both in a towing tank and in a cavitation tunnel, aimed at study the fluid-dynamics of an aeronautic drone-propeller in off-design conditions. Dynamometric, PIV and Stereo-PIV tests are carried out to evaluate the aeronautic propeller functioning in water and optimize it for amphibious missions. In particular, the forces are measured for different advance ratios J provided by varying both rotational regime and free stream velocity, in open water conditions (Towing tank tests) and in confined water (Cavitation tunnel tests). PIV and Stereo-PIV fields, acquired in the Cavitation tunnel, allow us to investigate the behaviour of the propeller in the water in a number of selected, operative conditions.

1. Introduction

Actually, drones represent one of the most promising technologies for the future of many sectors in terms of research, development and innovation.

Currently, many countries are investing in the use of drones in different areas in order to improve the effectiveness of human intervention, both in military and civilian sectors [1].

Drones can be the most efficient solution to replace and extend human presence in performing difficult or dangerous tasks and their adaptability to different conditions can be a key feature to have a reliable and flexible device [2]. An increasing number of studies focus on the technical difficulties of a drone that can change its configuration depending on the mission [3], [4]. Some of these tasks include the presence of water, such as inspecting oil pipelines, taking a bird's eye view of oil spills or monitoring the structural integrity of bridges, and surveying nature reserves. For these reasons, one of the most useful features the industrial market is attracted is the capability to manoeuvre in fluids with different properties, i.e. air and water. An amphibious drone shows very high scientific potential rather than industrial potential, as an understudied topic that can contribute in terms of innovation.

This research topic shows strong scientific potentiality but it also represents a great challenge from a technical point of view:

i) Amphibious drones must be able to maneuver efficiently in both water and air and safely ensure the achievement of mission objectives;
ii) Aeronautical propeller for drones in water must generate reverse thrust or braking force through an off-design rotation in off-design condition;
iii) Propeller rotational velocity in water is generally of one order of magnitude lower than the one in air so the engines must be properly designed for such a wide operational range.

Amphibious propeller design is one of the most complex scientific task. Many numerical methods were developed to investigate propeller design starting from the 1960s based on the lifting line theory [5]. With the advancement of computer performance the Computational Fluids Dynamics (CFD) methods became more accurately and with the modern numerical model like Blade element theory (BET), Blade element momentum theory (BEMT) [6], Free Vortex Method (FVM) [7]) it becomes possible to model very complex fluid flow problems. Numerical simulations allow to reduce drastically the time and cost of a propeller design but need some input parameter from experiments to produce accurate results. It is therefore crucial in order to develop new numerical method and improve their accuracy to carry on experimental campaigns that provide empirical data. The separation between the aerodynamic and the hydrodynamic propeller is no longer clear-cut since the first prototypes of amphibious drones are already developed and industrially available. In order to evaluate the performance of this new technology is therefore important and interesting analyse the drone propeller performances in an off-design condition like in the water. This knowledge can contribute in future to accelerate the design of innovative propellers for amphibious missions and to improve their numerical simulations. In this paper an experimental campaign aimed at quantifying the performance and characterizing the wake of an aeronautical propeller for drone in water is presented. A three-bladed, aeronautical propeller is experimentally characterized in water at the Institute of Marine Engineering in Rome, CNR-INM. In particular, the generated forces are acquired through a dynamometer for different advance ratios realized by varying both the rotational regime and the free stream velocity. Propeller wake measurements are performed using PIV and SPIV techniques.

2. Experimental Setup

The propeller under investigation is a KDE propeller, model no. KDE-CF155-TP 15.5” x 5.3, Triple-Edition Series. The propeller is made of Carbon-Fiber supplied for military, commercial and industrial applications, the assembled propeller reach a diameter of 393.32 mm.

Open water tests are conducted in the Umberto Pugliese Towing Tank (Figure 1), which is a rectilinear tank 13.5 m wide, 6.5 m deep and 470 m long; the carriage runs on the tank with a maximum speed of 15 m/s and an uncertainty of 1 mm/s.

	Rotation	Advance Ratio	Thrust	Torque
Quadrant 1	R	+ (carriage forward)	+	+
Quadrant 2	R	- (carriage backward)	+	+
Quadrant 3	L	- (carriage backward)	-	-
Quadrant 4	L	+ (carriage forward)	-	-

Table 1: Sign convention for the tests in the towing tank.

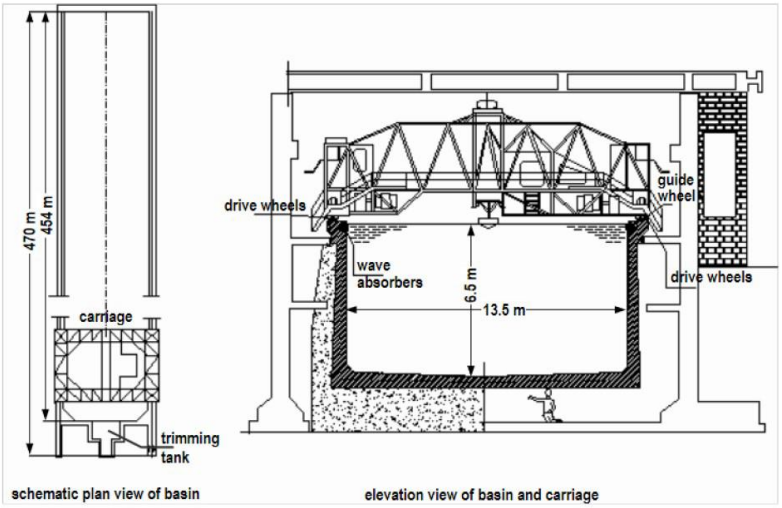

Figure 1: Schematic of the towing tank "Umberto Pugliese".

The experimental setup is sketched in **Figure *2***: the propeller is installed on the H29 dynamometer from Kempf & Remmers with full-scale values of 400 N for the thrust, 15 Nm for the torque and a maximum revolution speed of 60 RPS (Revolution Per Second).The thrust and torque time series are acquired with a sample frequency of 1000 Hz. The propeller is designed for a right rotational direction so the sign convention is determined as it's reported in **Table *1*** and represented in **Figure *5***.

The dynamometer is constrained to the carriage (that is not visualized) that runs at the advance speed V_A. According to the $ITTC$ Procedure and guidelines [8], the propeller axis was set at a distance of two propeller diameters from the free surface.

The global uncertainty, evaluated during the calibration of the instrument in dry conditions and on the past experience, is 0.39% for the thrust and 0.41% for the torque.

These tests allowed to measure the performances on all 4 quadrants of the propeller, in both pushing and braking conditions and in reverse thrust [10].

Additional tests were carried out in confined water conditions, in the Italian Navy cavitation tunnel (CEIMM), as sketched in **Figure *3***. The tunnel is a closed type cavitation tunnel with a square, rounded edges test section of 600x600x2600 mm^3, the maximum velocity is 12 m/s and the pressure is adjustable from 0.15 to 1.5 atm.

The propeller was installed on the J15 dynamometer from Kempf & Remmers with full scale values of 3000 N for the thrust, 150 Nm for the torque, a maximum revolution speed of 60 RPS and an accuracy of ±0.15%. The CEIMM tunnel offers undoubted advantages on the speed with both performances and PIV tests can be conducted; for this reason the performance results between the two facilities were compared in order to verify that the blockage effects are negligible.

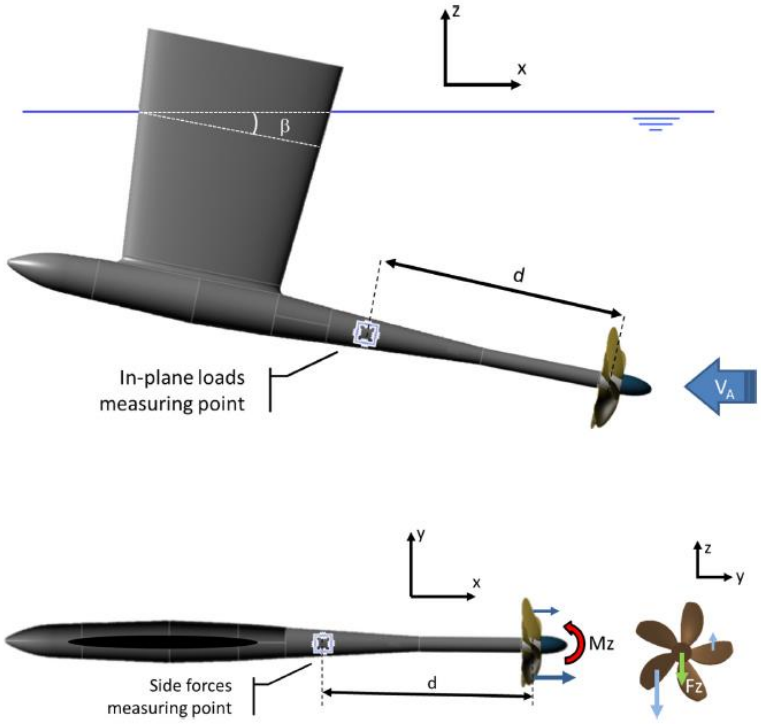

Figure 2: Open water tests setup.

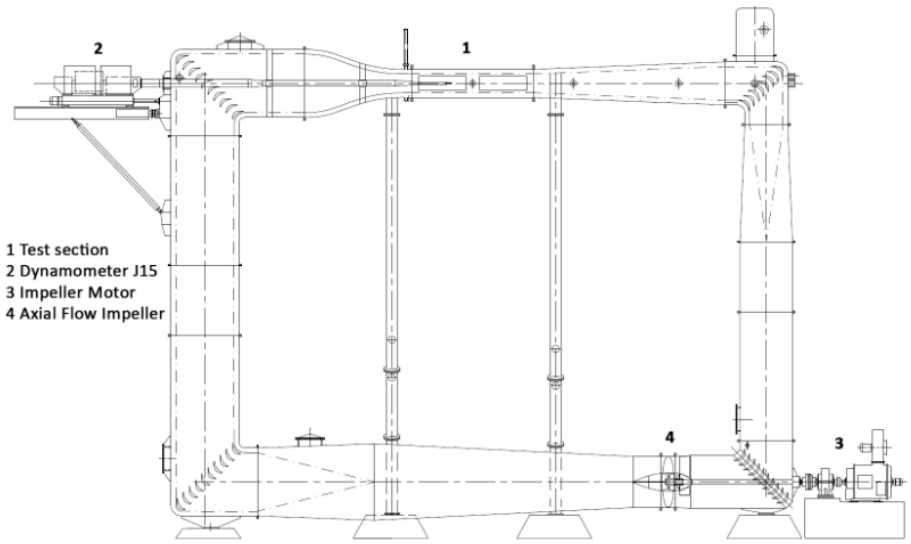

Figure 3: Schematic of the Italian Navy cavitation tunnel (CEIMM).

To perform PIV and Stereo-PIV measurement in the cavitation tunnel, setup was arranged as shown in **Figure *4***. For the 2D-PIV tests, the laser plane was aligned with the propeller axis and the undisturbed flow direction. A double frame 8 Mpx camera was installed orthogonal to the laser plane [11]. PIV images were acquired in phase locked angular steps of 10°. For each propeller phase, 500 images were acquired to ensure statistical convergence of the phase averages.

For the SPIV tests, to get a deeper insight on the blade wake, two 8 Mpx double frame cameras are installed in both sides of the tunnel in an asymmetric configuration to focus cameras on the right side blade using water-filled prisms [12], [13]. The laser plane is set orthogonal to the flow in the wake of a

blade and measurements are phase locked. SPIV is calibrated following Soloff [14] procedure with a dual plane target and a 3,3,1 polynomial degree respectively for x, y and z.

The laser used both in PIV and SPIV setup is a double-pulse Nd-YAG 200 mJ and the seeding particles are hollow-glass sphere of 40 μm diameter.

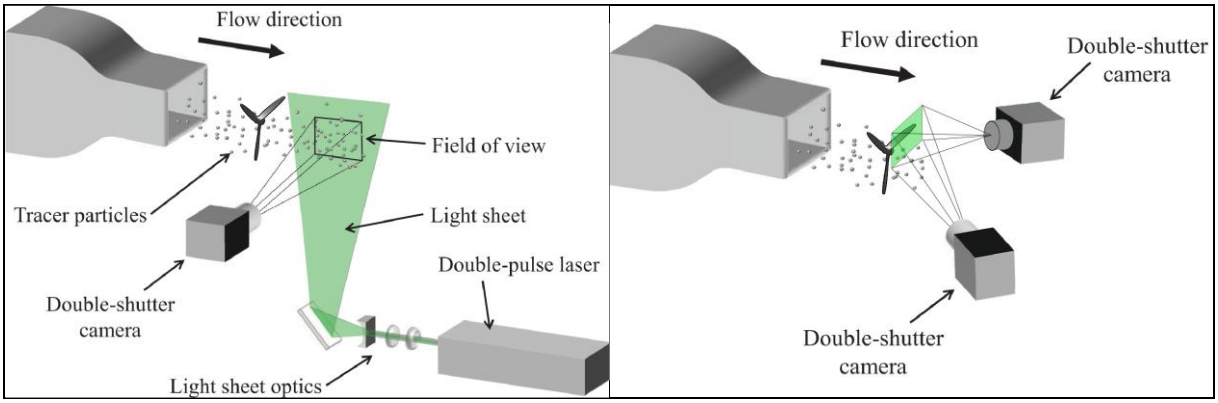

Figure 4: Schematic of the PIV (left) and Stereo-PIV (right) setup at cavitation tunnel.

3. Experimental results

3.1. Propeller performance

Thrust and torque measurements have been performed both in Towing Tank and CEIMM.
Test matrix of the experimental campaign is reported in **Table *2***. At Towing Tank tests are carried out at different rotational speeds, the four quadrants (see **Figure *5***) are acquired for a rotational speed of 3.87 RPS and the carriage velocities are identified in order to generate specific advance ratios (J) from about -0.7 to 0.7 with 0.1 step.
Propeller thrust and torque are reported in **Figure *5*** in terms of dimensionless coefficients (Kt and Kq) upon the advance ratio. Although the propeller has been designed and optimised to generate thrust in the air, its performance in the water is certainly of interest. In fact, despite the off-design application, it is noticeable the possibility to use the propeller for manoeuvring and to trim attitude and depth and also to operate both in braking and thrust reversing conditions. Tests are performed also at higher rotational speeds in order to investigate the propeller behaviour at different Reynolds numbers (Re_{07}).

Re_{07} is the Reynolds number evaluated at 70% of the propeller radius and is defined as:

$$Re_{07} = \frac{V_{07} c_{07}}{\nu}$$

where V_{07} is the propeller speed and c_{07} is the blade chord evaluated at 0.7R, ν is the kinematic viscosity of the water.

Tests in the cavitation tunnel are investigated spanning from 6 to 10 RPS. In order to quantify blockage effects. In particular, basin tests at 5.86 and tunnel tests at 6 RPS are compared: as shown in **Figure *6***, the performance curves are in good agreement proving a reduced blockage effects on the experimental data. In detail the efficiency curve is almost overlapped and the most relevant differences are evident for the K_T at higher J (>0.5) where the higher speeds increase the blockage effects.

The Reynolds number effect on the dimensionless coefficients is shown in **Figure *7***. The rotational regime was varied from 6 to 10 RPS corresponding to Re_{07} values from 160000 to 260000.

Approaching at Re_{07} equal to 250000 a condition of fully developed turbulence is obtained and the performances no longer increase with the Reynolds number, **Figure** *7* shows these effects comparing 6 RPS and 8-10 RPS rotational speeds.

As shown in **Figure** *7*, the propeller maximum efficiency is reached at J=0.35, with an increase of the maximum efficiency with the Reynolds number. It is important to note that although the propellers are not designed for propulsion in water, the maximum value assumed by their efficiency ranges from 0.55 to 0.63 (depending on the Reynolds number), this result is fundamental because it clearly shows the actual possibility of using propellers to operate in both air and water. It also prompts us to think that research aimed at optimising a propeller that has to operate in two fluids so different in terms of density and viscosity values is a road worth pursuing.

On the other hand, as expected, this kind of propeller offers high thrust only at low advance ratio. This issue can be ascribed to the low blade pitch angle related to the multirotor main mission: fixed-point flying.

Facility	Rotational Speed (RPS)	Test	Re_{07}	J range
Towing Tank	3.87	Performances and off-design	103434	from -0.7 to 0.7
Towing Tank	5.27	Performances	140852	from 0 to 0.7
Towing Tank	5.86	Performances	156621	from 0 to 0.7
CEIMM	6.00	Performances and PIV	160363	from 0.15 to 0.65
CEIMM	8.00	Performances	213817	from 0.15 to 0.65
CEIMM	10.00	Performances and PIV-SPIV	267271	from 0.15 to 0.65

Table 2: Test matrix.

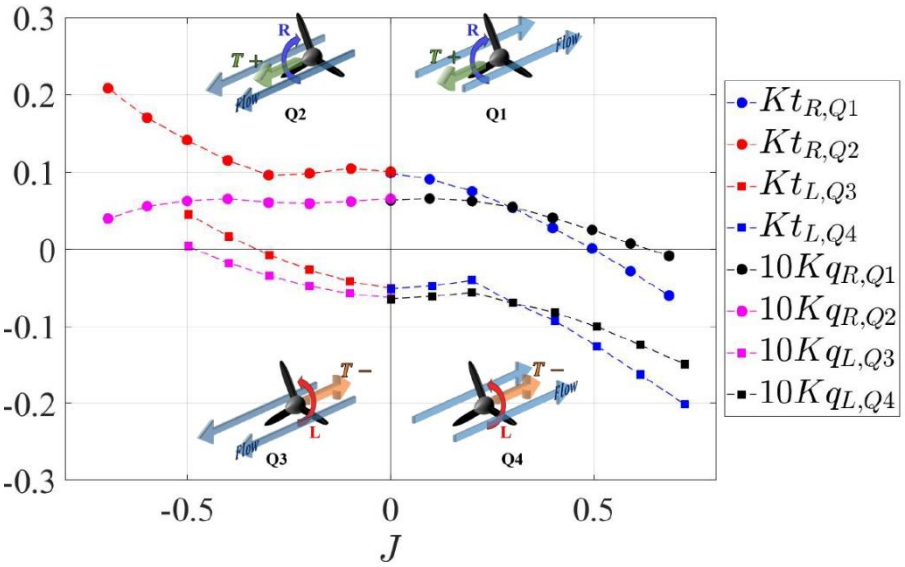

Figure 5: Towing tank off-design test.

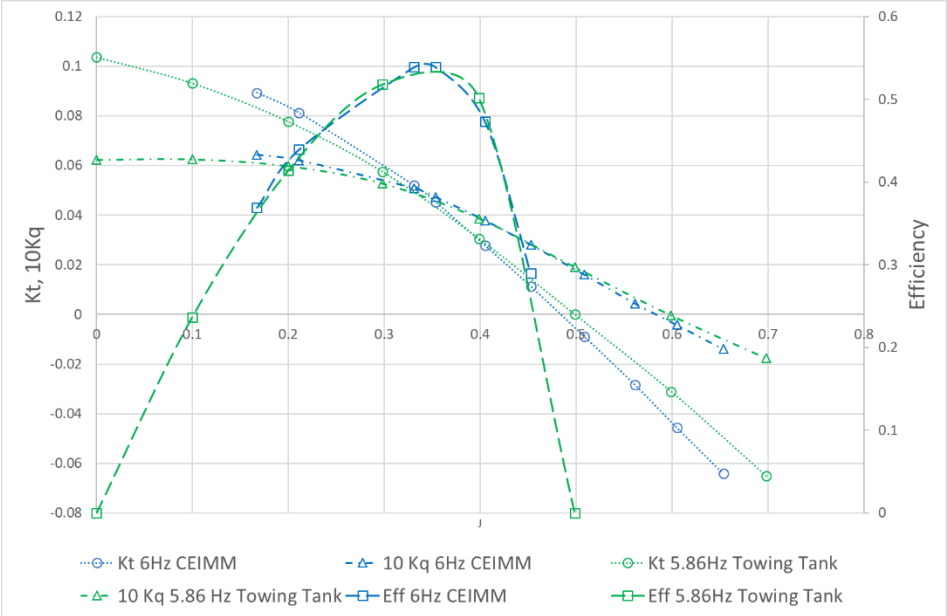

Figure 6: Towing tank and cavitation tunnel performance comparison.

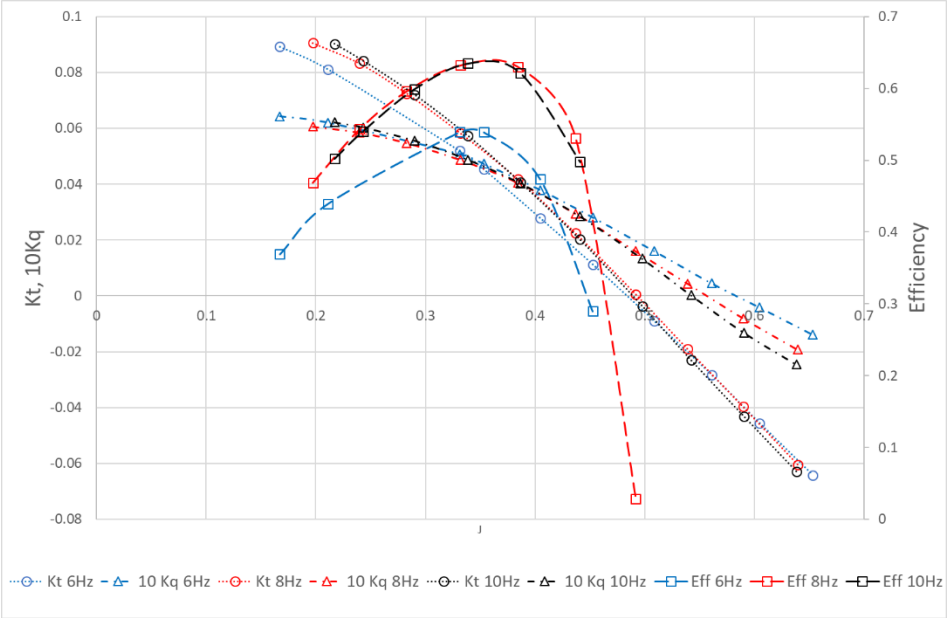

Figure 7: Cavitation tunnel performance tests: effects of the rotational speed.

3.2. PIV and Stereo-PIV results

PIV tests are aimed at measuring the propeller wake on the central plane. 500 PIV fields are acquired in phase locked conditions investigating a single blade passage (i.e. in relative angular coordinates, from 0° to 110°, in steps of 10°); 2 different rotational speeds (6 and 10 RPS) are measured at the maximum efficiency advance ratio (J=0.3), furthermore J=0.2 (high thrust) and J=0.65 (high braking) conditions are investigated at 10RPS.

Figure *8* and **Figure *9*** show respectively the dimensionless horizontal and vertical velocity fields for the measured conditions in correspondence of the propeller phase 0°. These figures show that, in the high thrust condition (J=0.21 10 RPS, top left), the flow downstream of the propeller is accelerated and is 2.5 times faster than U_0. In addition, the blade trails and the tip vortices are evident. The fields on the right (top and bottom) show the J=0.3 condition for 6 and 10 RPS, the dimensionless wake velocity is almost independent from the rotational speed except for the presence of more intense vortex traces at 10 RPS. The bottom left fields show the braking/energy harvesting condition (J=0.65), the propeller wake seems almost undisturbed with almost negligible velocity variations respect to the inflow velocity (U_0).

Figure *10* and **Figure *11*** show respectively the turbulent kinetic energy and the out-of-plane vorticity component fields. For the J=0.21 strong turbulent tip vortices and blade wakes can be observed. Both tip and root vortices are visible and a first interaction between vortices is already evident near the propeller (almost 0.5R). At J=0.3, vortices are weaker and in detail an interaction of vortices is visible only for 10 RPS condition at a distance of almost 1.5 R from the propeller plane, as previously seen the 6RPS condition shows weak vortices. At J=0.65, mainly a strong turbulence in the wake of the hub is present while tip vortices being outside of the field of view due to the wake expansion in radial direction that is evident in braking condition differently from the wake reduction occurring in thrusting condition.

The turbulent kinetic energy distribution, represented in

Figure *10* shows how the blade turbulence decreases faster downstream respect the hub turbulence.

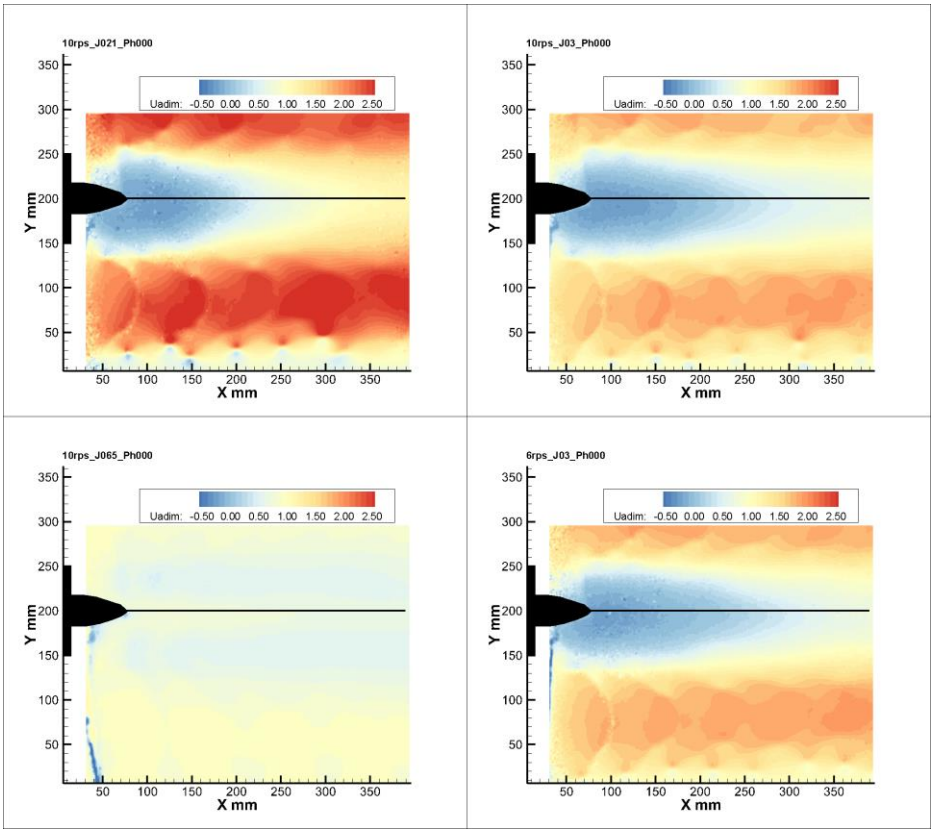

Figure 8: PIV results: Phase 0° dimensionless horizontal velocity.

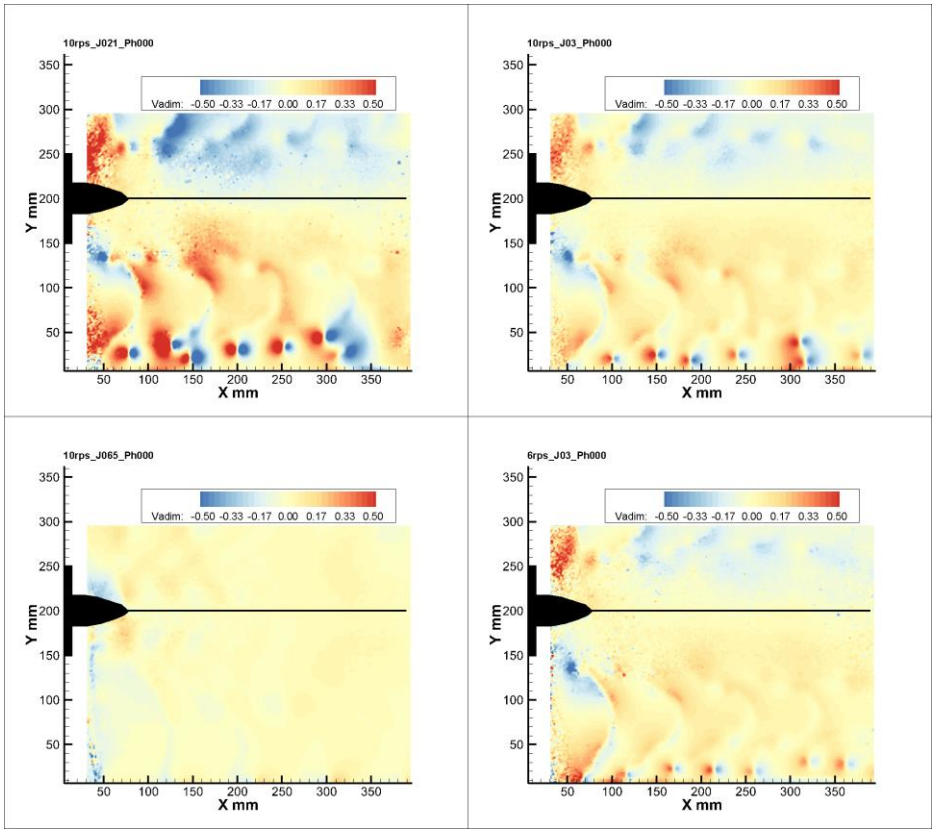

Figure 9: PIV results: Phase 0° dimensionless vertical velocity.

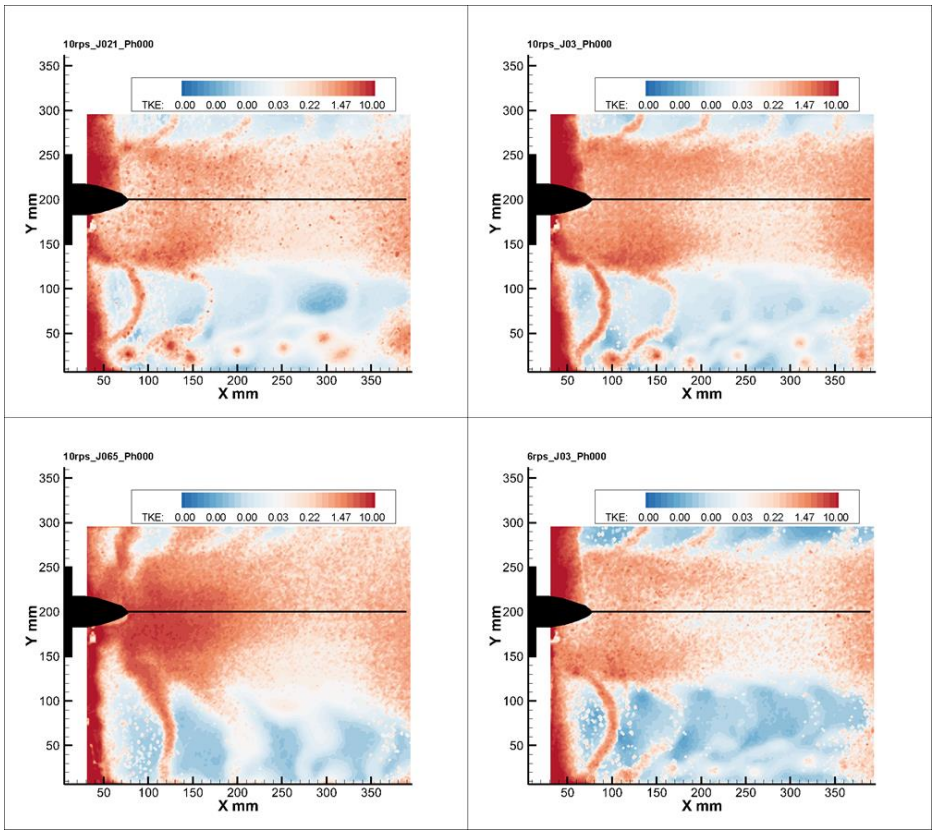

Figure 10: PIV results: Phase 0° Turbulent Kinetic Energy.

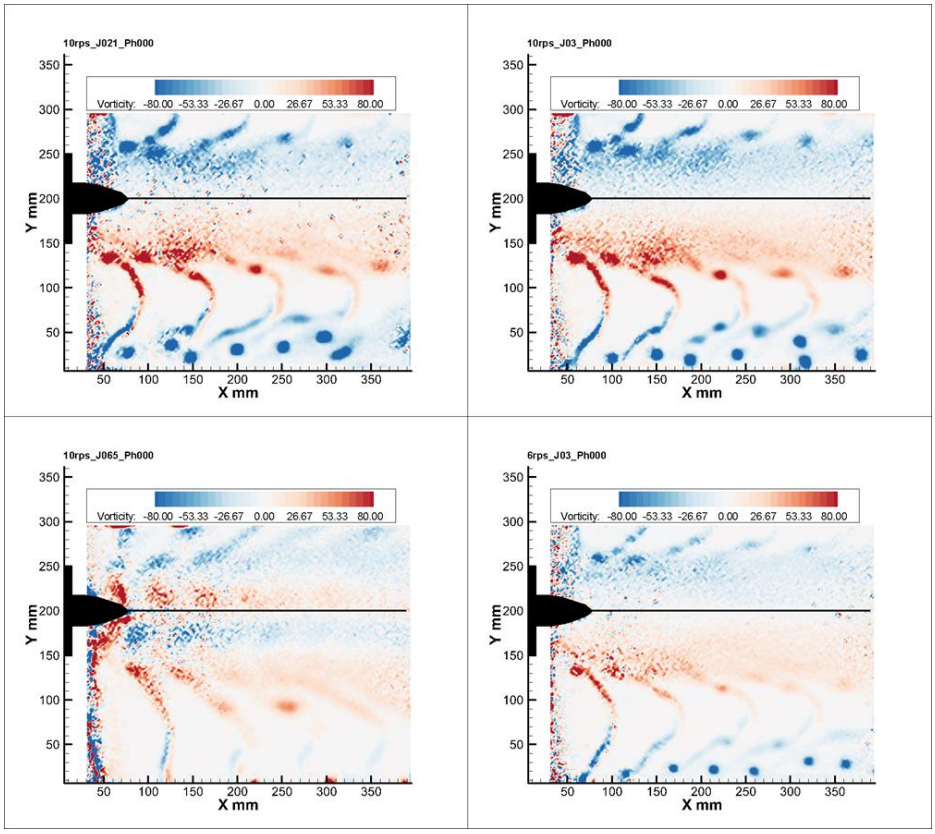

Figure 11: PIV results: Phase 0° out-of-plane vorticity component.

The SPIV campaign allows to study the cross-sectional view of the propeller blade wake, in particular in the J=0.65 condition, when the propeller is driven by the flow (braking/energy harvesting condition). Four measurement planes, orthogonal to the flow, have been imaged in the wake of a single blade of the propeller, placed at a distance ranging from 2 mm to 14 mm; the laser plane thickness was set as thin as possible (about 2mm) and planes was measured at 4 mm distance to reconstruct a volume in the wake of the blade, 500 phase locked images are acquired for each plane.

The measured planes allow to reconstruct a volume for evaluating all the components of vorticity tensor, the volume is thin and is 200x80x14 mm^3, the obtained resolution is about 3 mm in x and y and 4mm in z. **Figure *12*** shows the reconstructed volume and some vorticity iso-surfaces in the wake of the blade. The tip vortex structure and a tip roll up are reconstructed, moreover the trailing edge wake is evident and it is composed by 2 counter rotating vortices.

Figure *13* and **Figure *14*** show velocity and vorticity components in the measured planes in the wake of a single blade; the figures provide the structure of the tip vortex roll up (second row image 1 and 2), the first row show a trace of tip vortex formation with a gradient that starts from tip and moves to the top of the images. In details, the second row of the **Figure *13*** shows also the roll-up of the blade wake that bypass the leading edge in the measured braking condition.

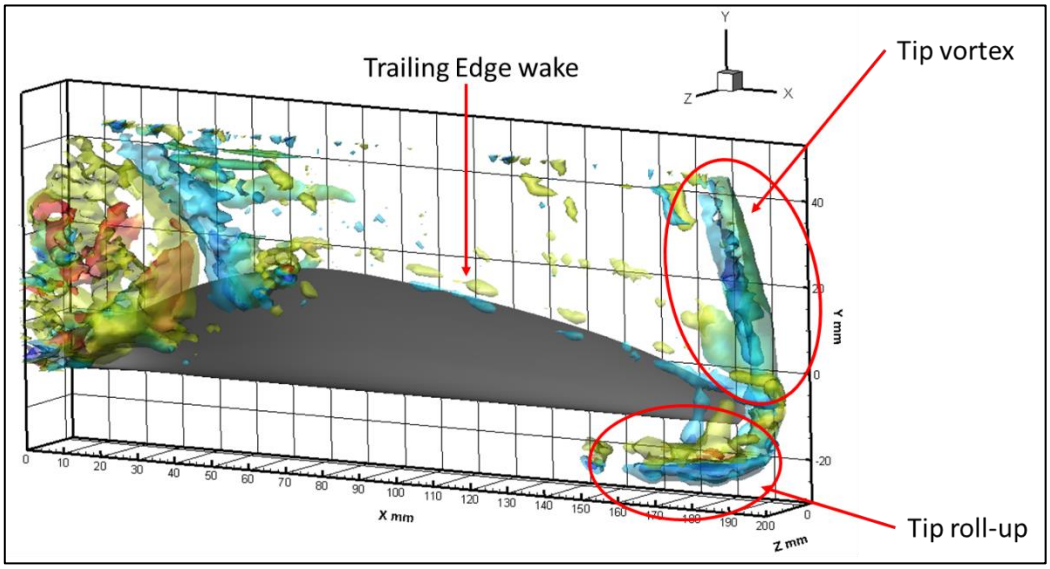

Figure 12: Blade wake volume: iso-vorticity surfaces.

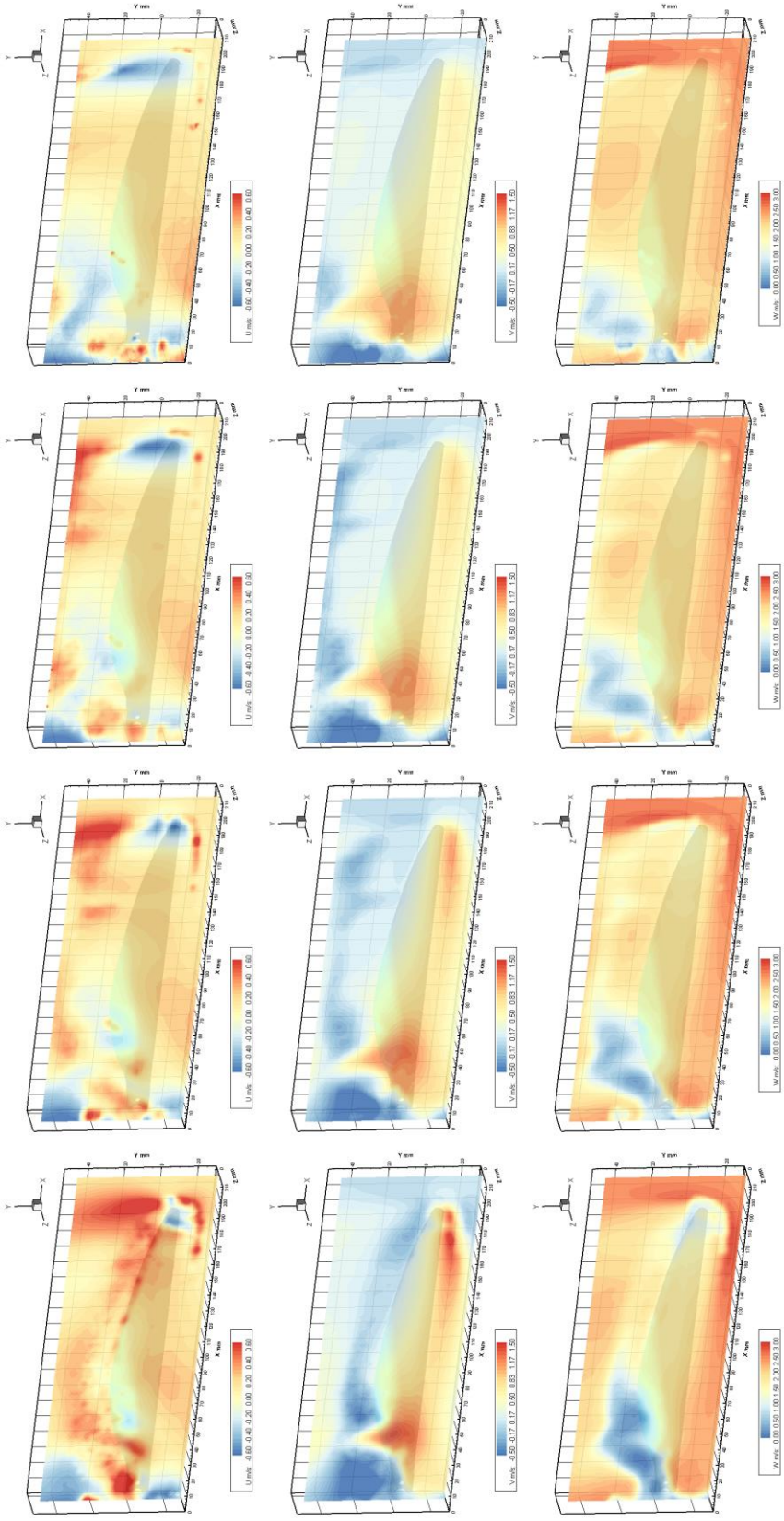

Figure 13: U, V and W velocity components in the wake of a blade at J=0.65.

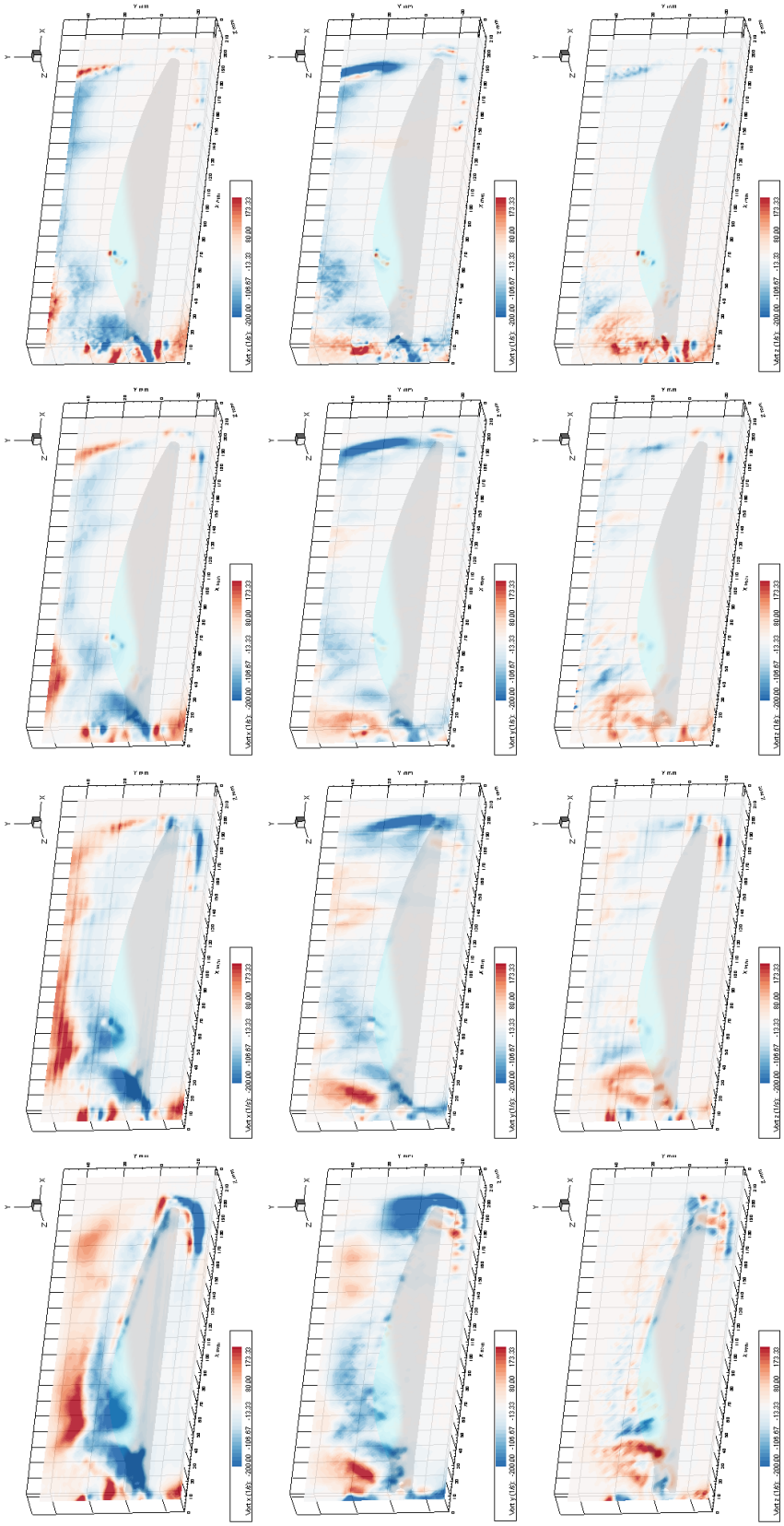

Figure 14: vorticity components in the wake of a blade at J=0.65.

References

[1] Suresh R, Ahamed Jasim A, Amal Nagdev OR, Binny Sabin B, Nagaraj V, and Jeyasimman D. Design and analysis of remotely amphibious drone. International Journal of Innovative Technology and Exploring Engineering (IJITEE), Volume-9 Issue-5, March 2020.
[2] Kuantama E, Craciun D, Tarca R. Quadcopter body frame model and analysis. Ann. Univ. Oradea, pages 71–74, 2016.
[3] Sharma P et al. Conceptual design and non-linear analysis of triphibian drone. Procedia computer science, 133:448–455, 2018.
[4] Brischetto S, Ciano A, Ferro CG. A multipurpose modular drone with adjustable arms produced via the fdm additive manufacturing process. Curved and Layered Structures, 3(1), 2016.
[5] Salvatore F, Testa C, Ianniello S, Pereira F. Theoretical modelling of unsteady cavitation and induced noise. In Proceedings of CAV 2006 Symposium, Wageningen, The Netherlands, 2006.
[6] Salvatore F, Greco L, Calcagni D. Computational analysis of marine propeller performance and cavitation by using an inviscid-flow bem model. In Second International Symposium on Marine Propulsors,(SMP2011), Hamburg, Germany, 2011.
[7] Javanmard E, Yari E, Mehr JA, Mansoorzadeh S. Hydrodynamic characteristic curves and behavior of flow around a surface-piercing propeller using computational fluid dynamics based on fvm. Ocean Engineering, 192:106445, 2019.
[8] ITTC, 2014. Quality System Manual-Recommended Procedures and Guidelines. Technical Report 7.5-0.2-0.3-0.2.1. 27nd International Towing Tank Conference (ITTC).
[9] Ortolani F, Mauro S, Dubbioso G, 2015. Investigation of the radial bearing force developed during actual ship operations. Part 1: Straight ahead sailing and turning maneuvers. Ocean Eng. 94, 67–87. http://dx.doi.org/10.1016/j.oceaneng.2014.11.032.
[10] Martellini E., Aloisio G, Grizzi S., Falchi M., Pagliaroli T., 2022, Hydrodynamic Performances of Aeronautical Propeller for Drones. Journal of Physics: Conference Series 2293, 012007. DOI: 10.1088/1742-6596/2293/1/012007
[11] Adrian RJ, Twenty years of particle image velocimetry, Experiments in Fuids 39, 159 – 169 , 2005
[12] Prasad AK, Adrian RJ, Stereoscopic particle image velocimetry applied to liquid flows, Experiments in fluids 15, 49 – 60 , 1993
[13] Zang W, Prasad AK, Performance evaluation of a Scheimpflug stereocamera for particle image velocimetry, Applied Optics 36, n°33, 8738 – 8744 , 1997
[14] Soloff SM, Adrian RJ, Liu ZC, Distortion compensation for generalized stereoscopic particle image velocimetry, Meas. Sci. Technol. 8, 1441 – 1454 , 1997